AGU PUBLICATIONS

Geophysical Research Letters

RESEARCH LETTER
10.1002/2015GL064885

Key Points:
- Eruptive sequence and intensity inferred from remote observations
- Moderate magnitude but high intensity for 2014 Kelud eruption
- Novel combination of seismic and infrasound to track long-range acoustic waves

Supporting Information:
- Supporting Information S1
- Table S1
- Table S2
- Figure S1
- Figure S2
- Figure S3
- Figure S4
- Figure S5

Correspondence to:
C. Caudron,
CCaudron@ntu.edu.sg;
corentin.caudron@gmail.com

Citation:
Caudron, C., B. Taisne, M. Garcés, L. P. Alexis, and P. Mialle (2015), On the use of remote infrasound and seismic stations to constrain the eruptive sequence and intensity for the 2014 Kelud eruption, *Geophys. Res. Lett.*, *42*, 6614–6621, doi:10.1002/2015GL064885.

Received 10 JUN 2015
Accepted 10 JUL 2015
Accepted article online 14 JUL 2015
Published online 19 AUG 2015

On the use of remote infrasound and seismic stations to constrain the eruptive sequence and intensity for the 2014 Kelud eruption

Corentin Caudron[1], Benoît Taisne[1], Milton Garcés[2], Le Pichon Alexis[3], and Pierrick Mialle[4]

[1]Earth Observatory of Singapore, Nanyang Technological University, Singapore, [2]Infrasound Laboratory, Hawaii Institute of Geophysics and Planetology, School of Ocean and Earth Science and Technology, University of Hawaii at Manoa, Honolulu, Hawaii, USA, [3]CEA/DAM/DIF, Arpajon, France, [4]CTBTO, Vienna, Austria

Abstract The February 2014 eruption of Kelud volcano (Indonesia) destroyed most of the instruments near it. We use remote seismic and infrasound sensors to reconstruct the eruptive sequence. The first explosions were relatively weak seismic and infrasound events. A major stratospheric ash injection occurred a few minutes later and produced long-lasting atmospheric and ground-coupled acoustic waves that were detected as far as 11,000 km by infrasound sensors and up to 2300 km away on seismometers. A seismic event followed ~12 minutes later and was recorded 7000 km away by seismometers. We estimate a volcanic intensity around 10.9, placing the 2014 Kelud eruption between the 1980 Mount St. Helens and 1991 Pinatubo eruptions intensities. We demonstrate how remote infrasound and seismic sensors are critical for the early detection of volcanic explosions, and how they can help to constrain and understand eruptive sequences.

1. Introduction

Volcanic eruptions radiate low-frequency (< 0.2 Hz in this study) infrasound and seismic waves which can travel over large distances from a volcanic center. These waves preserve valuable information of the eruption dynamics and chronology even when recorded hundreds to thousands of kilometers away and allow eruptions surveillance at safe distances from a volcano [*Fee et al.*, 2010; *Matoza et al.*, 2011a, 2011b; *Dabrowa et al.*, 2011; *Johnson and Ripepe*, 2011; *Fee and Matoza*, 2013]. Large volcanic explosions also generate enough low-frequency seismic energy to be recorded and analyzed by remote seismic stations [*Kanamori and Given*, 1982; *Kanamori et al.*, 1984; *Widmer and Zürn*, 1992; *Kanamori et al.*, 1994; *Shearer*, 1994; *Johnson and Malone*, 2007; *Lognonné et al.*, 2006; *Watada and Kanamori*, 2010].

Kelud volcano (Java Island, Indonesia, cyan triangle, Figure 1) produced one of the most powerful volcanic eruptions of the decade on 13 February 2014. The eruption began at night and injected ash up to 26 km above sea level [*Kristiansen et al.*, 2015]. In January 2014, the number of shallow and deep volcanic earthquakes detected by the local seismic network exponentially increased until 13 February [*Global Volcanism Program*, 2014]. This earthquake swarm triggered an increase in alert level from 3 to 4 (on the 1–4 scale, Centre for Volcanology and Geological Hazard Mitigation alert system) at 14:15 UTC (21:15 local time) on 13 February. At ~15:50 UTC, a major explosion destroyed the Closed-Circuit Television and four out of five seismic instruments deployed in the near field (<10 km) [*Global Volcanism Program*, 2014]. Subsequent seismicity was dominated by continuous tremor signals that saturated the remaining sensor.

We evaluate the eruptive chronology and constrain the Kelud eruptive sequence and intensity from remote (>200 km) infrasound and seismic data. We discuss how such signals could be generated and highlight the importance of using openly available seismic and infrasound data from stations located at safe distances from volcanic edifices.

2. Chronology of the Major Explosions

Several remote instruments detected the eruption. MTSAT-1R satellite identified exceptionally cold pixels [*Global Volcanism Program*, 2014], indicating a plume emission in the troposphere, at 16:09 UTC on 13 February

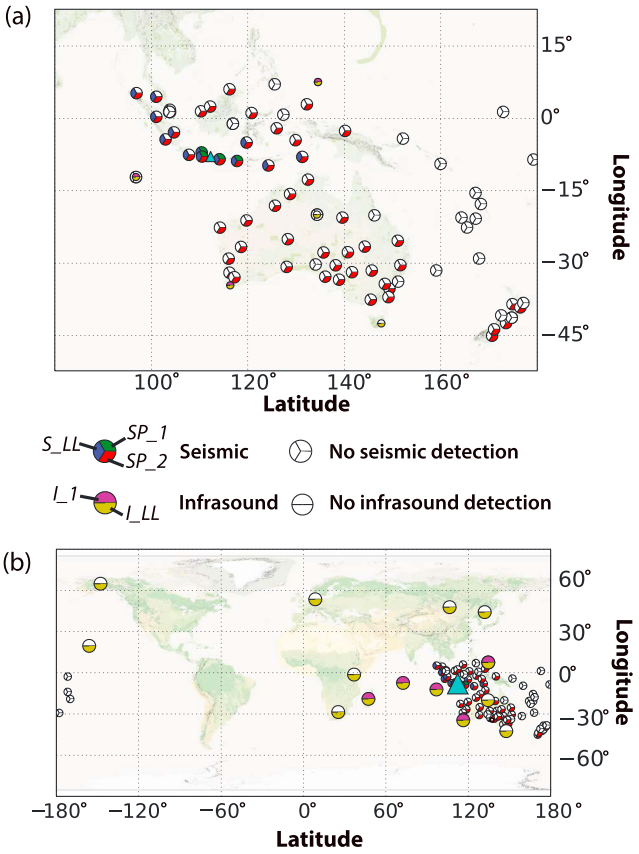

Figure 1. Kelud volcano (Central Java, Indonesia (7°56′00″S, 112°18′30″E)) (cyan triangle on Figures 1a and 1b). (a) Seismic detections: the pies are divided in three and correspond to the broadband sensors detections (IRIS and GEOFON networks) used in this study. Infrasound detections: the half pies are the infrasound stations (International Monitoring System (IMS) network). White colors correspond to a nondetection, green to the detection of S_P1, blue of S_LL, red of S_P2, magenta of I_1, and yellow of I_LL. Zoom on the region of interest (Figure 1a). (b) Global detections.

(Figure 2a). Ionospheric disturbances (Figure 2a) were detected by 37 stations of the Global Navigation Satellite Systems from 16:25 to ~19:00 UTC [*Nakashima et al.*, 2014].

Three distinct low-frequency (<0.2 Hz in this study) signals were observed using remote seismic data (Figure 2b). The first signal was only visible at four nearby seismic sites (S_P1, Figure 3), followed by a short-duration energetic signal observed up to ~7000 km (S_P2, Figure 3). Finally, a long lasting (S_LL) arrival could be tracked as far as West Sumatra (2300 km away, Figure 3). The difference in effective propagation speed (celerity) between S_P1-S_P2 and S_LL (Figure 3) is noteworthy and indicative of the two different wave types associated with the observations.

The volcanic eruption at Kelud volcano was automatically detected by the International Data Centre (IDC) of the Comprehensive Nuclear Test-Ban Treaty Organization (CTBTO) using infrasound arrays in the International Monitoring System (IMS). The subsequent reviewed analysis provided an extended list of infrasound signals associated with a series of eruptions. In the Reviewed Event Bulletin (REB) of the IDC, 5 detections were associated with a first event (I_1, Figures 2b and 3), whereas 14 detections correspond to a second signal of longer duration (I_LL, Figures 2b and 3). This is presently the largest number of IMS stations that has ever recorded a volcanic event. Using an experimental infrasound array located in West Java (Indonesia), *Hidayat* [2014] also recorded a short-duration impulsive signal followed ~15 min later by a long lasting high-amplitude signal.

All the stations detections are indicated on a map (Figure 1) and Table S1 in the supporting information summarizes the observations.

3. Data and Methods

During the last decade, seismic data have become increasingly available to the scientific community. The seismic data used in this study were downloaded from IRIS (Incorporated Research Institutions for Seismology, http://www.iris.edu/) and GEOFON seismic networks (http://geofon.gfz-potsdam.de/). Sensor responses between 0.001 and 10 Hz were deconvolved using the IRIS response files. Excepting the closest seismic stations, no distinct arrivals could reliably be observed in the raw and filtered waveforms (Figure S1). We manually picked seismic arrival times using spectrograms. For some stations, tectonic earthquakes were identified as the origin of low-frequency signals (Table S2 and Figure 4b). Due to the low-frequency content of the signals, spectrograms (Figures S2 and S3) were calculated using 10% cosine-tapered windows of 250 seconds (s), 500 s, and 1000 s durations with 90% overlap. The spectrograms' color scale varied for ease of picking. Short-duration seismic signals were picked using 250 s long time windows (S_P1 and S_P2, Figures S2 and S3),

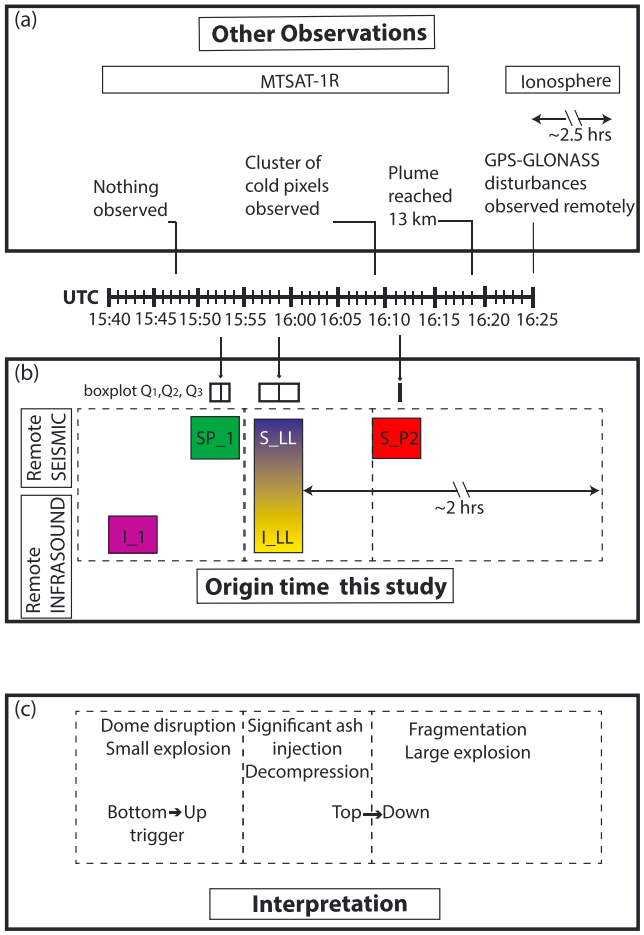

Figure 2. Timeline summarizing the observations and the eruptive sequence. (a) Other observations (ionospheric disturbances from *Nakashima et al.* [2014]). (b) This study: Q_1, Q_2, and Q_3 are the 25th percentile, the median, and the 75th percentile, respectively. (c) Interpretation.

while 500 and 1000 s long windows were used to pick longer-duration period signals (S_LL, Figure S2). For sustained seismic energy, the ending time was also measured (S_LL black rectangles, Figure S2). At some stations, this timing overlapped with tectonic earthquake wave arrivals (dashed box, BKNI station, Figure S2). In that case, the ending time corresponded to the tectonic earthquake arrival. Given the long window durations used for calculating the spectrograms, errors can be as large as 300 s. An error was associated to each reported time depending on its reliability (window length $\pm n$, where n is the number of pixels (1 pixel = window length) required to reliably pick a signal). The Inferno algorithm was used [*Garcès*, 2013] to estimate signal-to-noise ratio (SNR) energy when a risk of overlapping wave arrivals existed (i.e., for the stations nearby the volcano). The algorithm provides high-resolution multispectral analysis in logarithmic frequency space with time window autoscaling and is specifically designed to improve the temporal resolution of nonstationary signals.

The CTBTO IDC automatically processes in near real-time continuous infrasound recordings from the IMS stations. The system can associate signal detections at distances up to 60° from a source location. In order to better estimate the signal wave parameters, the recording for the associating IMS stations were systematically reprocessed using the Progressive Multi Channel Correlation (PMCC) method [*Cansi*, 1995]. PMCC used by IDC was configured with 18 logarithmic-spaced frequency bands, adapted from *Matoza et al.* [2013], with Chebyshev filters of order 2 between 0.07 and 4 Hz. Compared with the IDC automatic processing using 11 bands covering the same frequency range [*Brachet et al.*, 2009], this logarithmic-spaced configuration improves signal discrimination. The time window length varies in proportion to the period from 30 to 250 s and the window is time shifted by 10% of the window length. A typical result from a PMCC analysis is presented in Figure S4, for I39PW, in Palau.

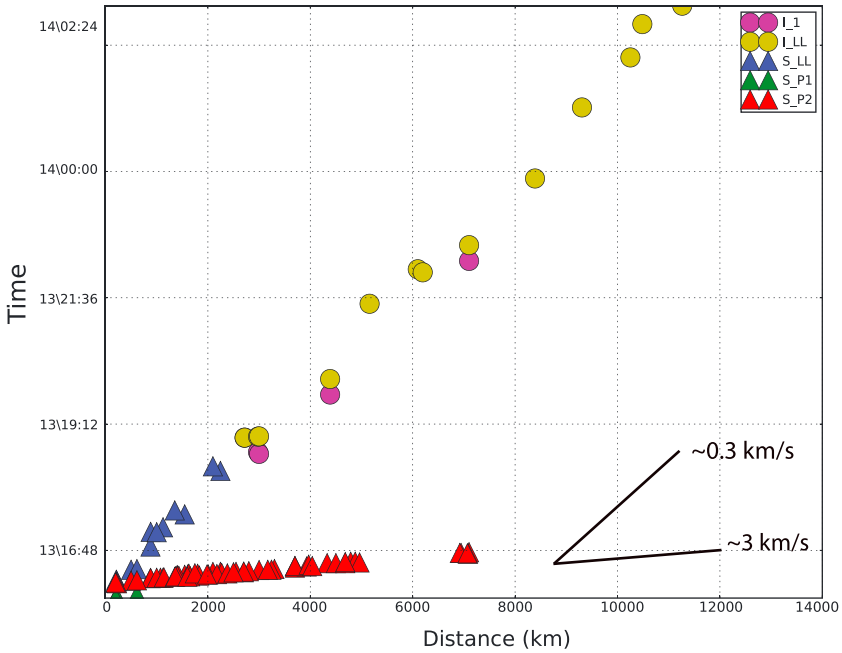

Figure 3. The different arrivals altogether as a function of the distance with respect to Kelud volcano.

4. Discussion

4.1. Observations

Different seismic and acoustic waves are apparent in the seismic record. Based on Figure 3, the range of arrival times for the second long-lasting infrasound signal (I_LL) clearly overlap with the arrival times of the long lasting (S_LL) seismic signal. Volcanic eruptions generate acoustic waves which can couple to the ground and be recorded by seismic instruments [e.g., *Braun and Ripepe*, 1993; *Johnson and Malone*, 2007]. We postulate that I_LL and S_LL are associated to the same acoustic source. A Bayesian approach is used to estimate the best combination of origin times and wave celerities to fit the observations. We account for errors on the arrival

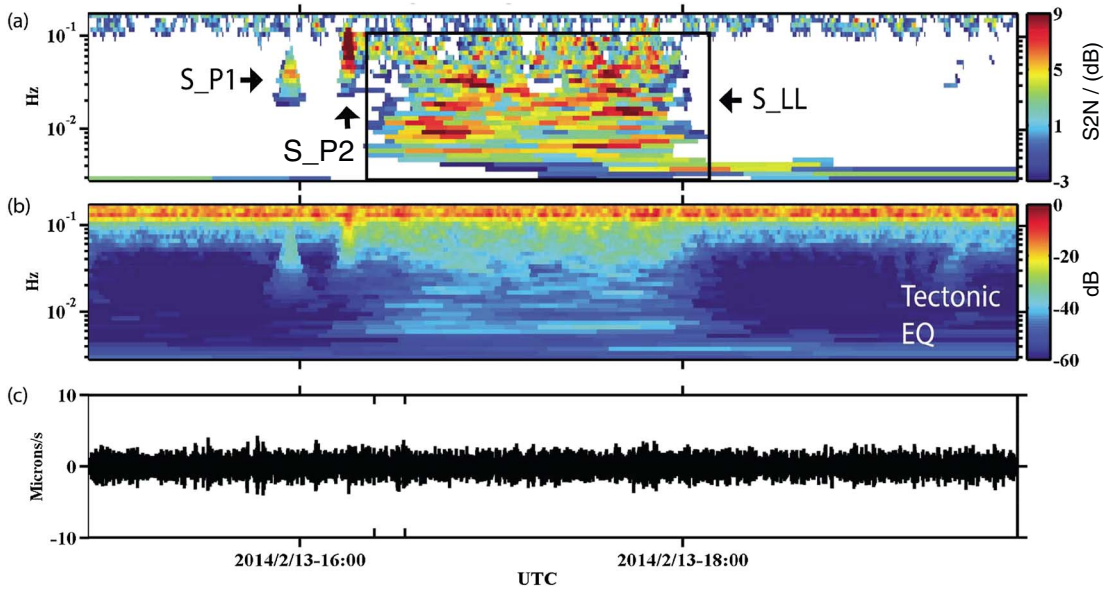

Figure 4. Signal recorded at GE-UGM (Yogyakarta, Central Java, Indonesia, 198 km from Kelud volcano). (a) Spectrogram of signals having a high signal-to-noise ratio (SNR, in dB, where the noise is considered as the energy averaged over the record at each frequency band). (b) Raw spectrogram. (c) Corresponding seismogram. Figures 4a and 4b are computed using sixth octave bands and 1/f window scaling with a 75% overlap (dB referenced to 1 micron/s). A tectonic earthquake (EQ) is indicated in Figure 4b.

times for S_P1 and S_P2 during the picking procedure, whereas for S_LL and I_LL the uncertainty is assumed to be proportional to the distance and values for celerities ranging between 260 and 350 m/s [*Brown et al.*, 2002]. The inversion results for origin times and celerities are as follows: (1) S_P1: 15:52:29 UTC (first quartile: 15:51:46, third quartile: 15:53:10 UTC) and 1.84 km/s (first quartile: 1.45 km/s, third quartile: 2.42 km/s), (2) S_LL and I_LL: 15:58:43 UTC (first quartile: 15:56:53, third quartile: 16:00:33 UTC) and 267 m/s (first quartile: 255 m/s, third quartile 281 m/s), (3) S_P2: 16:11:21 UTC (first quartile: 16:11:12, third quartile: 16:11:29 UTC) and 3.41 km/s (first quartile: 3.36 km/s, third quartile: 3.46 km/s), and (4) I_1: 16:12:41 UTC (first quartile: 15:51:45, third quartile: 16:36:08 UTC) and 386 m/s (first quartile: 314 m/s, third quartile: 515 m/s).

Apart from I_1, the origin times and celerities are well constrained and match our expectations for the postulated common source. Specifically, the I_LL origin time is in good agreement with the results presented by *Hidayat* [2014] using an experimental infrasound array located ~600 km to the west of Kelud volcano. Since infrasound propagation is unlikely to change between I_1 and I_LL, we disregard the poorly constrained origin time and celerity for I_1. Following this study and *Hidayat* [2014] results, this signal probably occurred at ~15:43, or ~15 min before I_LL. These results permit an estimate of the eruptive chronology and sequence (Figure 2b).

I_1 corresponds to a brief low-amplitude impulsive signal of low-amplitude, consistent with a small eruption [*Dabrowa et al.*, 2011] and was captured by five IMS infrasound stations (Table S1). An explosion (S_P1) was then detected at nearby seismometers only (GE-JAGI, GE-SMRI, GE-UGM ,and GE-PLAI, Table S1). These volcanic signals possibly correspond to relatively weak phreatic explosions and/or dome disruption.

The long-lasting acoustic signal was recorded as far as Alaska (~11,200 km, I_LL, Table S1) by the microbarometer arrays of the IMS network, whereas the farthest seismometer with a clear signal was ~2200 km (S_LL, Table S1) away from Kelud volcano. Remote infrasound detections are relatively common [e.g., *Dabrowa et al.*, 2011] as sound in the stratospheric waveguide propagates with low attenuation. This signal could possibly be related to long-duration atmospheric oscillations of the volcanic jet or plume [*Matoza et al.*, 2009]. At Redoubt Volcano, low-frequency infrasound signals are coincident with high-altitude ash emissions [*Fee et al.*, 2013]. At Soufrière Hills Volcano, Montserrat, *Ripepe et al.* [2010] attributed the infrasonic signals to initial oscillations of the rising ash plume after lava dome collapse. In any case, this signal indicates the beginning of ash injection into the atmosphere corresponding to the major eruption. Its low frequency, long duration, and high amplitude (Figure S4) suggest stratospheric ash injection [*Garcés et al.*, 2008]. Ten minutes later (16:09 UTC, Figure 2a), the first cold pixels associated with a significant plume were observed by MTSAT-1R satellite [*Global Volcanism Program*, 2014].

Ground-coupled acoustic waves were detected and associated to Mount St. Helens (USA) eruption [*Johnson and Malone*, 2007]. However, they were recorded within 350 km of the source. This study suggests an efficient coupling between the acoustic and seismic wave until ~2300 km (blue pies, Figure 1a). The few exceptions (e.g., on the east side of Indonesia, close to Papua) correspond to seismic stations with low ambient noise level. The seismic stations which detected the acoustic signal (Figure 1a) do not suggest any important azimuthal constrain on the detection. At frequencies <0.8 Hz, the attenuation is less sensitive to the strength and direction of the prevailing stratospheric winds [*Le Pichon et al.*, 2012]. For propagation ranges larger than 200 km, while the attenuation is roughly constant when $V_{eff-ratio} > 1$ (where $V_{eff-ratio}$ is a dimensionless parameter defined by the ratio between the effective sound speed at 50 km altitude and the sound speed at the ground level), it strongly increases with frequency when upwind propagation occurs (from 0.1 to 3.2 Hz, the attenuation increases by ~80 dB at a distance of 1000 km from the source). At higher frequency, eastern stations would not have detected any signal. Considering the low-frequency content of the recorded signal, the wave could also be ducted by the thermosphere in all directions, as it was the case for the 1991 Pinatubo eruption [*Tahira et al.*, 1996]. The long lasting wave arrivals suggest stratospheric celerities around 280 m/s to the west of Kelud and slightly lower to the east, which could indicate thermospheric propagation. This is in agreement with later arrivals on seismic and acoustic stations to the east of Kelud volcano.

While the first seismic signal was a regional event (200–600 km, estimated M_S of 2.3), the last seismic event of short duration was detected at much greater ranges (200–7000 km, estimated M_S of ~4.7). Most of the seismic stations which did not detect this seismic signal appeared to be noisy at the expected time of arrival. Low-frequency waves were also detected at teleseismic distances by seismometers after extremely explosive eruptions: in 1980, Mount St. Helens (USA) [*Kanamori and Given*, 1982], in 1982, El Chichon (Mexico) [*Widmer and Zürn*, 1992; *Shearer*, 1994], in 1991, Mount Pinatubo (Philippines) [*Widmer and Zürn*, 1992].

By using the long lasting signal duration in the infrasound and seismic records (Figure S5) and the total volume of 0.2–0.3 km^3 dense rock equivalent [*Nakada et al.*, 2014], we estimate the intensity of the eruption to ~10.8–11.0 (following $I = \log_{10}$ mass eruption rate + 3, where I is the intensity and the mass eruption rate is in kg/s [*Pyle*, 2000]). Remote infrasonic and seismic stations permit an assessment of the eruptive intensity from the signal duration. Although of smaller magnitude ($M = 4.3–4.5$, where magnitude = log_{10} (erupted mass) − 7, with the erupted mass in kg [*Pyle*, 2000]), the Kelud 2014 eruption was of higher intensity than the 1980 Mount St. Helens ($M = 4.8$ and intensity = 10.3), but much lower than the 1991 Pinatubo ($M = 6.0$, intensity = 11.6) eruption. The ash plume reached 19 km and 35 km of elevation during Mount St. Helens and Pinatubo eruptions, respectively, while a maximum height of 26 km was measured following the 2014 Kelud eruption [*Kristiansen et al.*, 2015]. Although outside the scope of this paper, it would be interesting to compare the band-passed infrasound and seismic records of these historical eruptions. The intensity, as a measure of the violence of mass injection, is a useful real-time impact metric for monitoring and hazard assessment. As demonstrated in this case study, a small magnitude but intense eruption, such as the 2014 Kelud eruption, can rapidly impact habitats, communities, and flight routes.

4.2. Interpretation

A key observation for Kelud 2014 eruption concerns the sequence itself (Figure 2b). The first volcanic events were not detected by satellites and include a brief infrasound signal followed by a weak seismic event. The first episode likely disrupted the dome plugging the conduit, therefore, suggesting a "bottom-up" trigger that could have been induced by magma mixing. The acoustic signal, also recorded on seismometers, probably occurred when the plug capping the conduit was breached and volcanic material could be freely injected into the atmosphere. This may correspond to the onset of a decompression that induced magma fragmentation [*Alidibirov and Dingwell*, 1996]. The second seismic signal was only later recorded (Figure 2b). Following *Jeffery et al.* [2013], a prominent storage region lies in the midcrust (~10 km) and several magma storage zones are distributed throughout the uppermost crust (<10 km depth). *Melnik and Sparks* [2002] estimate that a fragmentation front can propagate over a few kilometers. Our results suggest an upper apparent fragmentation speed ~15 m/s (assuming the deepest reservoir lied at maximum 10 km). This range is in good agreement with experimental results [*Spieler et al.*, 2004] for similar overpressures (~7 MPa, $P = h_{\mathrm{dome}}\, g\, \rho$, with h_{dome} and ρ derived from *Jeffery et al.* [2013]).

Although all eruptions are bottom-up in terms of magma ascent, highly dangerous explosive phases can also be triggered by "top-down" processes (1980 Mount St. Helens, USA, 2006 Soufrière Hills, Montserrat, and 2010 Merapi, Indonesia [*Pallister et al.*, 2014; *Voight et al.*, 2006; *Surono et al.*, 2013]). In the Kelud 2014 eruption case, the most explosive event was triggered by a top-down process, probably following the dome unloading. The 1919 eruption followed a similar sequence although in place of a dry dome [*Caudron et al.*, 2012], a crater lake of 40 million m^3 overlaid the conduit at that time [*Kemmerling*, 1921]. The first event which blew off the lake was minor and was followed by the main explosion, also of short duration (<10 h). In 1990, a phreatic eruption followed by minor phreatomagmatic eruptions preceded the large Plinian eruption by less than an hour [*Vandemeulebrouck et al.*, 2000]. The main phase only lasted for a few hours.

5. Conclusions

The eruption that occurred on 13 February 2014 at Kelud volcano was one of the most intense event of the decade. The first explosion destroyed most of the instruments deployed in the near field and the remaining seismic data were saturated due to intense eruption tremor. Hence, the eruptive sequence of this large volcanic event could not be easily monitored and constrained by the local network.

By analyzing seismic and infrasound data acquired at distances greater than ~200 km, a detailed eruptive sequence can be obtained. First, a weak infrasound signal was followed by a small magnitude seismic event. A long-lasting acoustic signal, concurrent with major stratospheric ash injection, was then globally recording by infrasound arrays (up to 11,000 km) and more locally (up to 2200 km) by seismic instruments due to efficient ground coupling. A seismic event was finally recorded by seismometers, as far as 7000 km away from the volcano. Although of moderate magnitude (4.3–4.5), the intensity (~10.8–11.0) places the 2014 Kelud eruption between the 1980 Mount St. Helens and 1991 Pinatubo eruptions (10.7 and 11.0). The results may suggest a bottom-up followed by a more explosive top-down trigger and are in agreement with experimental fragmentation speeds (<15 m/s) for similar overpressures (~7 MPa).

This study illustrates the growing importance of openly available data collected at safe distances from a volcano to detect and characterize eruptions from remote regions with sparse ground-based instrument network. Since remote seismic and infrasound data can be streamed in real time, they may be critical in volcanic crisis situations when the local network is destroyed.

Acknowledgments

We wish to thank the Editor and reviewers who significantly improved the quality of the manuscript. All seismic data used in this study are available on the web (IRIS and GEOFON networks). The facilities of IRIS Data Services, and specifically the IRIS Data Management Center, were used for access to waveforms, related metadata, and/or derived products used in this study. IRIS Data Services are funded through the Seismological Facilities for the Advancement of Geoscience and EarthScope (SAGE) Proposal of the National Science Foundation under cooperative agreement EAR-1261681. Some infrasound data are available from IRIS. Others are available upon request. The seismic data have been processed using Obspy [*Krischer et al.*, 2015]. This paper benefited from LATEX, Matplotlib (Hunter 2007), and Cartopy. The authors are grateful to the CTBTO and IMS station operators for guaranteeing the high quality of the infrasound data analyzed in this study. M. Garces' contribution was funded in-part by the Consortium for Verification Technology under the Department of Energy National Nuclear Security Administration, award DE-NA0002534. This work comprises Earth Observatory of Singapore contribution 102. This research is supported by the National Research Foundation Singapore and the Singapore Ministry of Education under the Research Centres of Excellence initiative.

The Editor thanks two anonymous reviewers for their assistance in evaluating this paper.

References

Alidibirov, M., and D. B. Dingwell (1996), Magma fragmentation by rapid decompression, *Nature*, *380*(6570), 146–148.

Brachet, N., D. Brown, R. Le Bras, Y. Cansi, P. Mialle, and J. Coyne (2009), Monitoring the Earth's atmosphere with the global IMS infrasound network, in *Infrasound Monitoring for Atmospheric Studies*, edited by A. Le Pichon, E. Blanc, and A. Hauchecorne, pp. 77–118, Springer, Netherlands.

Braun, T., and M. Ripepe (1993), Interaction of seismic and air waves recorded at Stromboli Volcano, *Geophys. Res. Lett*, *20*(1), 65–68.

Brown, D. J., C. N. Katz, R. Le Bras, M. P. Flanagan, J. Wang, and A. K. Gault (2002), Infrasonic signal detection and source location at the Prototype International Data Centre, *Pure Appl. Geophys.*, *159*(5), 1081–1125.

Cansi, Y. (1995), An automatic seismic event processing for detection and location: The P.M.C.C. Method, *Geophys. Res. Lett.*, *22*(9), 1021–1024, doi:10.1029/95GL00468.

Caudron, C., A. Mazot, and A. Bernard (2012), Carbon dioxide dynamics in Kelud volcanic lake, *J. Geophys. Res.*, 117, B05102, doi:10.1029/2011JB008806.

Dabrowa, A., D. Green, A. Rust, and J. Phillips (2011), A global study of volcanic infrasound characteristics and the potential for long-range monitoring, *Earth Planet. Sc. Lett*, *310*(3), 369–379, doi:10.1016/j.epsl.2011.08.027.

Fee, D., and R. S. Matoza (2013), An overview of volcano infrasound: From Hawaiian to Plinian, local to global, *J. Volcanol. Geotherm. Res.*, *249*, 123–139, doi:10.1016/j.jvolgeores.2012.09.002.

Fee, D., A. Steffke, and M. Garces (2010), Characterization of the 2008 Kasatochi and Okmok eruptions using remote infrasound arrays, *J. Geophys. Res.*, *115*, D00L10, doi:10.1029/2009JD013621.

Fee, D., S. R. McNutt, T. M. Lopez, K. M. Arnoult, C. A. Szuberla, and J. V. Olson (2013), Combining local and remote infrasound recordings from the 2009 Redoubt Volcano eruption, *J. Volcanol. Geotherm. Res.*, *259*, 100–114, doi:10.1016/j.jvolgeores.2011.09.012.

Garcés, M., et al. (2008), Capturing the acoustic fingerprint of stratospheric ash injection, *Eos Trans. AGU*, *89*(40), 377–378.

Garcès, M. A. (2013), On infrasound standards. Part 1: Time, frequency, and energy scaling, *InfraMatics*, *2*, 13–35.

Global Volcanism Program (2014), Report on Kelut (Indonesia): February 2014, in *Bulletin of the Global Volcanism Network Global Volcanism Program 39:02*, edited by R. Wunderman, pp. 8–21, Smithsonian Institution, Washington, D. C.

Hidayat, M. (2014), Infrasound monitoring in Indonesia, paper presented at Infrasound Technology Workshop 2014, Vienna, Austria, Oct.

Hunter, J. D. (2007), Matplotlib: A 2D graphics environment, *Comput. Sci. Eng.*, *9*, 90–95.

Jeffery, A. J., et al. (2013), The pre-eruptive magma plumbing system of the 2007–2008 dome-forming eruption of Kelut volcano, East Java, Indonesia, *Contrib. Mineral. Petrol.*, *166*(1), 275–308.

Johnson, J. B., and S. D. Malone (2007), Ground-coupled acoustic airwaves from Mount St. Helens provide constraints on the May 18, 1980 eruption, *Earth Planet. Sci. Lett.*, *258*(1), 16–31, doi:10.1016/j.epsl.2007.03.001.

Johnson, J. B., and M. Ripepe (2011), Volcano infrasound: A review, *J. Volcanol. Geotherm. Res.*, *206*(3), 61–69.

Kanamori, H., and J. W. Given (1982), Analysis of long-period seismic waves excited by the May 18, 1980, eruption of Mount St. Helens-A terrestrial monopole?, *J. Geophys. Res.*, *87*, 5422–5432, doi:10.1029/JB087iB07p05422.

Kanamori, H., J. W. Given, and T. Lay (1984), Analysis of seismic body waves excited by the Mount St. Helens eruption of May 18, 1980, *J. Geophys. Res.*, *89*, 1856–1866, doi:10.1029/JB089iB03p01856.

Kanamori, H., J. Mori, and D. G. Harkrider (1994), Excitation of atmospheric oscillations by volcanic eruptions, *J. Geophys. Res.*, *99*, 21,947–21,961, doi:10.1029/94JB01475.

Kemmerling, G. L. L. (1921), *De uitbarsting van den G. Keloet in den nacht van den 19den op den 20sten Mei 1919*, Landsdrukkerij, Weltevreden, Stellenbosch.

Krischer, L., T. Megies, R. Barsch, M. Beyreuther, T. Lecocq, C. Caudron and J. Wassermann (2015), ObsPy: A bridge for seismology into the scientific Python ecosystem, *Comput. Sci. Discovery*, *8*(1), 014003.

Kristiansen, N., A. Prata, A. Stohl, and S. Carn (2015), Stratospheric volcanic ash emissions from the 13 February 2014 Kelut eruption, *Geophys. Res. Lett.*, *42*, 588–596, doi:10.1002/2014GL062307.

Le Pichon, A., L. Ceranna, and J. Vergoz (2012), Incorporating numerical modeling into estimates of the detection capability of the IMS infrasound network, *J. Geophys. Res.*, *117*, D05121, doi:10.1029/2011JD016670.

Lognonné, P., J. Artru, R. Garcia, F. Crespon, V. Ducic, E. Jeansou, G. Occhipinti, J. Helbert, G. Moreaux, and P.-E. Godet (2006), Ground-based GPS imaging of ionospheric post-seismic signal, *Planet. Space Sci.*, *54*(5), doi:10.1016/j.pss.2005.10.021.

Matoza, R. S., D. Fee, M. A. Garcés, J. M. Seiner, P. A. Ramón, and M. A. H. Hedlin (2009), Infrasonic jet noise from volcanic eruptions, *Geophys. Res. Lett.*, *36*, L08303, doi:10.1029/2008GL036486.

Matoza, R. S., A. Le Pichon, J. Vergoz, P. Herry, J.-M. Lalande, H.-I. Lee, I.-Y. Che, and A. Rybin (2011a), Infrasonic observations of the June 2009 Sarychev Peak eruption, Kuril Islands: Implications for infrasonic monitoring of remote explosive volcanism, *J. Volcanol. Geotherm. Res.*, *200*(1), 35–48, doi:10.1016/j.jvolgeores.2010.11.022.

Matoza, R. S., et al. (2011b), Long-range acoustic observations of the Eyjafjallajökull eruption, Iceland, April–May 2010, *Geophys. Res. Lett.*, *38*, L06308, doi:10.1029/2011GL047019.

Matoza, R. S., M. Landès, A. Le Pichon, L. Ceranna, and D. Brown (2013), Coherent ambient infrasound recorded by the International Monitoring System, *Geophys. Res. Lett.*, *40*, 429–433, doi:10.1029/2012GL054329.

Melnik, O., and R. Sparks (2002), Modelling of conduit flow dynamics during explosive activity at Soufrière Hills Volcano, Montserrat, *Geol. Soc. London, Mem.*, *21*(1), 307–317.

Nakada, S., M. Yoshimoto, F. Maeno, M. Iguchi, A. Zaenudin, and M. Hendrasto (2014), Recent two distinct eruptions at Sinabung and Kelud, Indonesia, Abstract V33E-06 presented at 2014 Fall Meeting, AGU, San Francisco, Calif., 15–19 Dec.

Nakashima, Y., K. Heki, A. Takeo, M. N. Cahyadi, and A. Aditiya (2014), Ionospheric disturbances by volcanic eruptions by GNSS-TEC: Comparison between Vulcanian and Plinian eruptions, Abstract NH33C-05 presented at 2014 Fall Meeting, AGU, San Francisco, Calif., 15–19 Dec.

Pallister, J., S. Andreastuti, W. McCausland, and R. Wessels (2014), "Bottom-up" versus "top-down" triggering of eruptions, Cities on Volcanoes 8, Jogyakarta, Indonesia, Sept.

Pyle, D. (2000), Sizes of volcanic eruptions, in *Encyclopedia of Volcanoes*, vol. 1, edited by H. Sigurdsson, pp. 263–269, Academic Press, San Diego, Calif.

Ripepe, M., S. De Angelis, G. Lacanna, and B. Voight (2010), Observation of infrasonic and gravity waves at Soufrière Hills Volcano, Montserrat, *Geophys. Res. Lett.*, *37*, L00E14, doi:10.1029/2010GL042557.

Shearer, P. M. (1994), Global seismic event detection using a matched filter on long-period seismograms, *J. Geophys. Res.*, *99*, 13,713–13,725, doi:10.1029/94JB00498.

Spieler, O., D. Dingwell, and M. Alidibirov (2004), Magma fragmentation speed: An experimental determination, *J. Volcanol. Geotherm. Res.*, *129*(1), 109–123.

Surono, P., et al. (2013), The 2010 explosive eruption of Java's Merapi volcano–A "100-year"event, *J. Volcanol. Geotherm. Res.*, *241–242*, 121–135.

Tahira, M., M. Nomura, Y. Sawada, and K. Kamo (1996), Infrasonic and acoustic-gravity waves generated by the Mount Pinatubo eruption of June 15, 1991, in *Fire and Mud: Eruptions and Lahars of Mount Pinatubo, Philippines*, edited by C. Newhall and R. Punongbayan, pp. 601–612, Philipp. Inst. of Volcanol. and Seismolog., Univ. of Washington Press, Quezon City, Seattle and London.

Vandemeulebrouck, J., J.-C. Sabroux, M. Halbwachs, N. Surono, N. Poussielgue, J. Grangeon, and J. Tabbagh (2000), Hydroacoustic noise precursors of the 1990 eruption of Kelut Volcano, Indonesia, *J. Volcanol. Geotherm. Res.*, *97*(1), 443–456.

Voight, B., et al. (2006), Unprecedented pressure increase in deep magma reservoir triggered by lava-dome collapse, *Geophys. Res. Lett.*, *33*, L03312, doi:10.1029/2005GL024870.

Watada, S., and H. Kanamori (2010), Acoustic resonant oscillations between the atmosphere and the solid earth during the 1991 Mt. Pinatubo eruption, *J. Geophys. Res.*, *115*, B12319, doi:10.1029/2010JB007747.

Widmer, R., and W. Zürn (1992), Bichromatic excitation of long-period Rayleigh and air waves by the Mount Pinatubo and El Chichon volcanic eruptions, *Geophys. Res. Lett.*, *19*(8), 765–768, doi:10.1029/92GL00685.